ACERP: Vol. 1, No. 2, (Summer 2015) 34-39

Advanced Ceramics Progress

Research Article

Journal Homepage: www.acerp.ir

# Wear Behavior in Micro and Nano-Structured WC-9Co-0.7VC Cemented Carbide Produced by Rapid Hot Press Sintering

H. Sedaghati*, M. Tamizifar

*Department of Metallurgy and Materials Engineering, , Iran University of Science and Technology, Tehran, Iran*

*PAPER INFO*

*Paper history:*
Received 14 April 2015
Accepted in revised form 01 November 2015

*Keywords*:
WC–Co
Cemented carbide
Nano-structured hard-metal
Hot pressing
Wear

*ABSTRACT*

Wear behavior in micro and nano-structured cemented carbide was compared. Tungsten carbide, cobalt and vanadium carbide powders were milled by high energy planetary ball mill. Microscopic observation and crystallite size calculation showed that crystallite size and particle size of powders were achieved less than 100 nano meters after milling at 15:1 ball powder ratio during 20 h. Micro and nano-sized WC-9Co-0.7VC powders were compacted at 30 MPa pressure and sintered at 1300 °C for 2 mints in rapid hot pressing process. Metallographic study by scanning electron microscopy demonstrated that WC particle size remained in nano-scale after sintering. Sliding friction test was carried out in a pin-on-disk system. The results showed that further wear resistance in nano-structured hard-metal was because of changes in the mechanism of material removal. It must be said that wear mechanism in hard-metals was abrasion / adhesion. It seemed that in micro-structured hard-metal, abrasion was more effective than adhesion, and vice versa in nano-structured hard-metal.

## 1. INTRODUCTION

Cemented carbides are groups of the most applicable advanced materials for their special properties [1]. Cemented carbides with ultra-fine WC grain size have a good combination of several mechanical properties [2]. Recent works have shown that, in nano-structured cemented carbides all properties such as hardness, fracture toughness, wear resistant, transverse rupture strength can be improved [3]. In many industrial applications especially machining industry, wear resistance is significant [4].

Co content and WC grain size are two important parameters that have main effects on wear behavior of cemented carbides. Research results show that wear rate increase with Co content and WC grain size, but these findings are relevant to the micro-structured hard metals [5].

Wear mechanisms of micro-structured cemented carbide have been already investigated; however there are few researches about nano-structured cemented carbides [6-11]. Previous researches about wear properties of WC-Co composites mainly appertain to micro-structured hard metal. The various factors affecting wear behavior such as WC grain size, Co content and mean free path in micro structured and ultrafine structured hard metal, have been studied but there are very low published resources about wear mechanisms in nano-structured hard-metal up to now.

In this research, sliding wear response of micro and nano-structured cemented carbides was studied. Morphology of the worn surfaces of WC–Co cemented carbides were determined by scanning electron microscopy. Differences between wear mechanisms in micro and nano-structured cemented carbide were also studied.

*Corresponding Author's Email: sedaghati@iust.ac.ir (H. Sedaghati)

## 2. EXPERIMENTAL PROCEDURES

### 2.1. Preparation of nano-size WC-CO-VC powder

WC (99.6%), Co (99.4%) and VC (99.8%) with average particle size of 0.22, 0.52 and 0.1 μm were respectively used as starting materials (Figure 1). WC-9Co-0.7VC powders and cemented carbide balls (10, 20 and 30 mm in diameter) mixed at ethanol were sealed in WC hard-metal vial in a glove box containing inert atmosphere of argon. The process of milling was continued for 20 h on a high energy planetary ball mill (Retsch PM400–MA type) with the selected rotation velocity of 200 rpm and 1:-3 rotation ratio. The powders were milled at 15:1 ball powder ratio (BPR). After milling, they were dried in a vacuum oven (Heraeus vaccutherm 660M) at 100 °C for 24 h. Using this method, nano-sized powders were prepared.

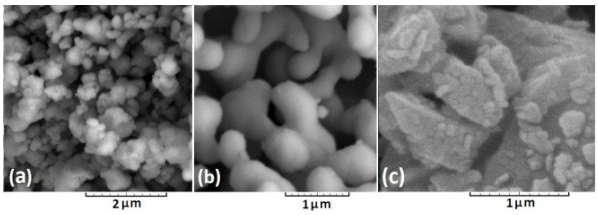


**Figure 1.** SEM images of starting powders (a) WC, (b) Co and (c) VC.

In order to produce micro-structured hard-metal specimen, primary micro-sized WC, Co and VC powders were just milled in dry condition for 2 h for the purpose of homogenization.

**2.2. Preparation of micro and nano-structured cemented carbides** Sintering was carried out by rapid hot pressing process (KPF-RHP 1500). The powders were compacted in a cylindrical graphite die at pressure of 30 MPa and heated by induction simultaneously. Sintering process was optimized by the variation of time and temperature, and finally, consolidation at 1300°C for 2 mints of soaking time was chosen for the best sintering condition. Heating schedule was shown in Figure 2. Average heating rate was more than 800 °C $min^{-1}$. The bulk with dimensions of 12 mm × 12 mm × 4 mm was consolidated (Figure 3). The sintered samples were grinded and polished by 3 and 1 µm diamond pastes. These specimens were etched by Murakami solution for 1 min.

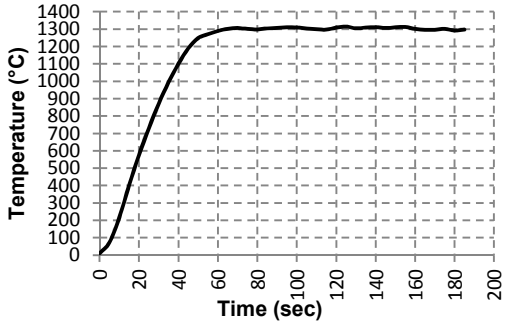


**Figure 2**. Heating curve in rapid hot pressing process

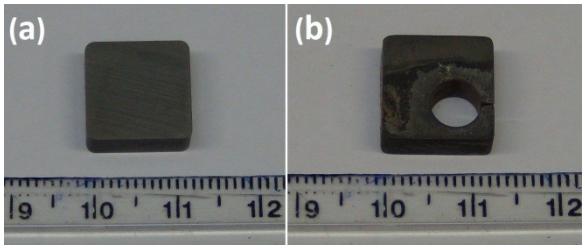


**Figure 3.** Image of one sample after (a) rapid hot pressing process and (b) separating wear sample.

**2.3. Hardness and densification** Hardness was measured by Vickers hardness (HV30) with 30 kg load (Wolpert Die Tester 7021 apparatus) by using ASTM B0294-92R01 method. Density of the sintered samples was determined by Archimedes method. Relative bulk densities of the sintered samples were measured by ASTM B311−93 standard.

**2.4. Sliding wear test** Sliding friction tests were carried out using pin–on–disk system following ASTM G0099-04A procedure. Hard metal pins were separated from samples by wire cutting process. Standard hardened steel (63 HRC) was used as a material for the counter face. Main application of this hard metal is making a nanostructured cutting tools for machining hard steels. Hence, counter face has made of martensitic steel. The tests were performed using contact load of 50 N, sliding velocity of 1 m $s^{-1}$, sliding distance of 1000 m and wear track radius of 13.8 mm. All the tests were conducted at room temperature and the noise parameters such as environmental temperature and humidity were controlled in the same conditions. Friction coefficient and weight loss of the worn samples were calculated from difference in the mass of specimens before and after each test, using a digital balance with scale of 0.1mg. Wear test was repeated three times for each sample.

**2.5. Metallography** Powders, structures and wear tracks of the bulk samples were analyzed by field emission scanning electron microscopy (MIRA II FEG–SEM) and transmission electron microscopy (Philips EM 208). The powders were dripped onto stand covered with gold after being shocked by ultrasonic waves in ethanol for preparing SEM samples.

## 3. RESULT AND DISCUSSION

**3.1. Specifications of nano-sized powder and nano-structured cemented carbides** Figure 4. indicates nano-particles morphology of WC-9Co-0.7VC after milling based on FE-SEM and TEM observations. It is obvious that milling process with 15:1 BPR for 20 h produced enough energy for converting micro-sized WC particles into nano-sized agglomerated powder. XRD pattern as shown in Figure 5. was used to determine the crystallite size being obtained by Williamson-Hall method [12].

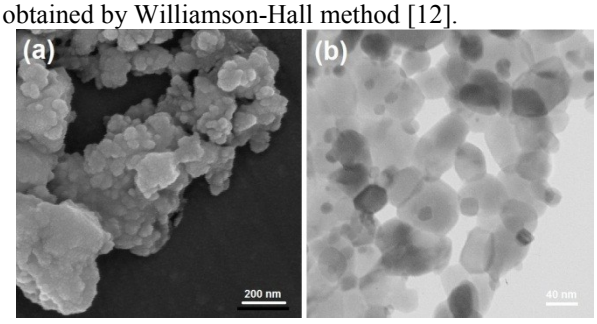


**Figure 4.** Microscopic observation of WC-9Co-0.7VC powder after milling (a) FE-SEM image and (b) TEM image.

Nano powders were annealed in drying process and wear used as standard samples. In order to estimate the

peak broadening due to the effect of particle size, as well as the effect of non-uniform (inhomogeneous) strain, Williamson-Hall method as described in the Eq. (1) is commonly used.

$$B_r \cos\theta = \frac{\lambda}{D} + 4\varepsilon \sin\theta \quad (1)$$

Where (Br) is the peak width (integral width) resulting from the size of crystallites (D) and the amount equivalent to inhomogeneous strain (4ε).

The integral width showing the width of rectangular which is the same as peak heights and has same area is computed for more than two diffraction peaks and then the graphic relation between (Br cos θ) and (sin θ) is drawn. Analysis is often carried out by using ($B_{1/2}$) FWHM instead of the integral width. Since a linear correlation is usually observed between these two quantities, a slope of the line gives the (4ε) value for inhomogeneous strain and an intersection with the (Br cos θ) axis corresponds to the reciprocal of the size of crystallites (D).

Statistical calculations of grain size by Full Width Half Maximum (FWHM) method and standard deviation values showed that average size of the crystallite was about 59 nm.

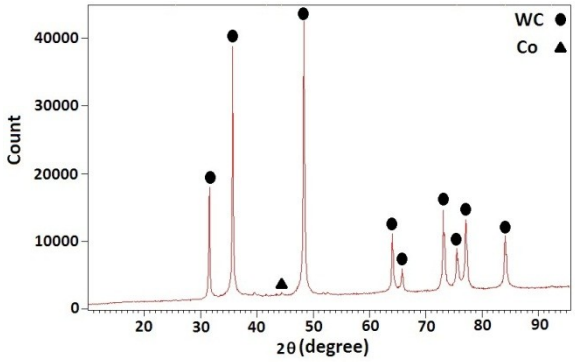


**Figure 5.** XRD pattern for WC-9Co-0.7VC powder after milling.

High heating rate in rapid hot pressing process led to inhibition of solution and precipitation mechanism in cemented carbide; therefore, growth of WC grains was prevented in Nano-structured hard-metal specimen. WC grain size in Nano-structured sample, as mentioned in Table 1. remained less than 100 Nano meters. On the other hand, sufficient temperature, pressure and soaking time led to high densification in both micro and Nano-structured hard-metal specimens. Average grain size of WC grains by quantitative metallography in CLEMEX VISION software. In Figure 6. it can be seen that grain size for micro-structured sample, is 841±76 nm and according to Figure 7. average grain size for nanostructured sample, is 41±9 nm.

Comparison of hardness in micro and nano-structured cemented carbides in Table 1. represented obvious differences while both samples have adequate densification.

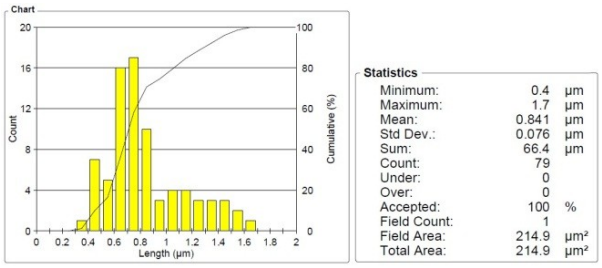


**Figure 6.** Results for determination of average WC grain size in micro-structured sample, by Clemex software.

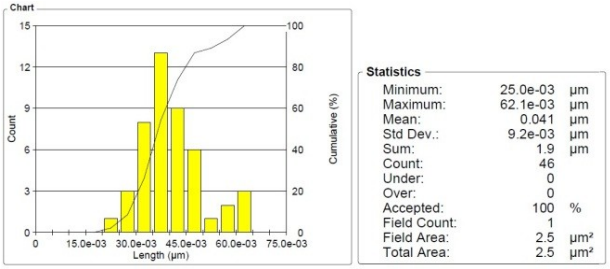


**Figure 7.** Results for determination of average WC grain size in nano-structured sample, by Clemex software.

Metallographic images of cross section in micro and nano-structured hard-metal are given in Figure 8a and b respectively. As a result of suitable hardness and densification in nano-structured hard-metal bulk specimen, satisfactory certainty existed about efficiency and sufficiency of sintering.

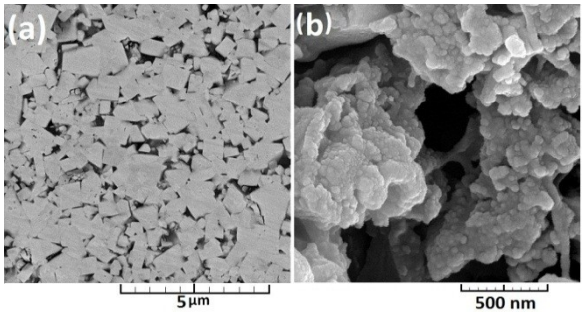


**Figure 8.** SEM images of (a) micro-structured and (b) nano-structured samples.

### 3.2. Wear results and mechanisms

Numerical wear results are shown in Table 1. It can be expected that wear behavior in micro-structured hard-metal was completely different from that in nano-structured hard-metal. Wear test for micro and nano structured samples was repeated three times. In any way; the shape of sample will not be corrupted after the wear according to Figure 9. In wear test, weight loss in both samples (pin and counter face) can be seen.

Mean friction coefficients for micro and nano-structured hard-metal specimens were 0.49 and 0.77 respectively. But, weight loss in the micro-structured specimen was more than 2.5 times of the nano-structured sample. Since weight loss was observed in both pin and disc, it can be concluded that material transfer has negligible effect on wear process; therefore, EDX analysis from

worn surface didn't reflect any important information, one of these analysis can be seen in Figure 10.


**Figure 9.** Image of nanostructured pin after wear test.

Friction coefficients were continuously recorded for WC-9Co-0.7VC/steel couples during the tests and mean values of friction coefficients in micro and nano-structured specimens are shown in Figures 11a and b respectively. These graphs demonstrated that coefficient of friction for micro-structured hard-metal/steel couple was lower than nano-structured hard-metal/steel couple. The difference in friction coefficient curves may reflect differences in the mechanism.

**TABLE 1.** Specification and numerical wear results in micro and nano-structured samples.

| Sample | Composition | Average WC grain size (nm) | Relative density ($g/cm^3$) | Hardness (HV30) | Weight loss (mg) | Average friction coefficient |
|---|---|---|---|---|---|---|
| Micro-structured | WC-9Co-0.7VC | 841±76 | 99.4 | 1310 | 3.7 | 0.49 |
| Nano-structured | WC-9Co-0.7VC | 41±9 | 99.1 | 1743 | 1.4 | 0.77 |

According to Figure 11a. in micro-structured sample the friction coefficient abruptly increased during the first 30 m of sliding and then gradually decreased to a "steady–state" value after about 1000 m of sliding; but, in nano-structured hard-metal, this flow was reversed. According to Figure 11b. in nano-structured cemented carbide, wide deviation from mean value of friction coefficient graph showed intensive involvement between the surfaces. However, high mechanical properties and suitable integrated micro-structure prevented demolition.

In the initial stage of wear testing, a burnishing wear process established a smooth wear track surface by plough away the surface asperities or roughness. As the wear proceeded further, wear track became smoother and coefficient of friction was fixed at a steady level.

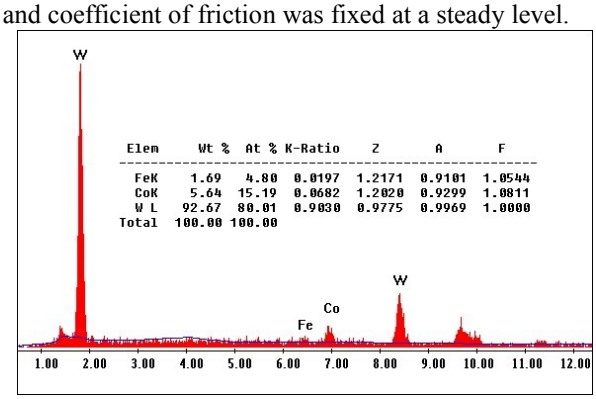


**Figure 10.** Large area EDS analysis from wear surface in nanostructured sample.

Microscopic study of the wear track on micro-structured hard-metal surface was performed, as given in Figure 12. As mentioned before, two factors influenced wear behavior in hard-metals: Co content and WC grain size. In micro-structured hard-metal, smooth surface indicated that asperities were plastically deformed during the test. Some surface porosity was probably caused by the fact that some carbide particles were torn out from material after 1 km run. The binder phase was partially removed from WC grains by combination of adhesion and micro-abrasion. The steady-state stage of wear occurred when sufficient binder was removed and in the following, released WC particles from the surface were entrapped and crushed. Figure 12a. represent that long cracks (arrows) grew parallel and plumb with wear direction and huge pieces were torn off from the surface. Then, deep holes remained on the surface. According to Figure 12b. WC particles can be clearly seen in white circle.

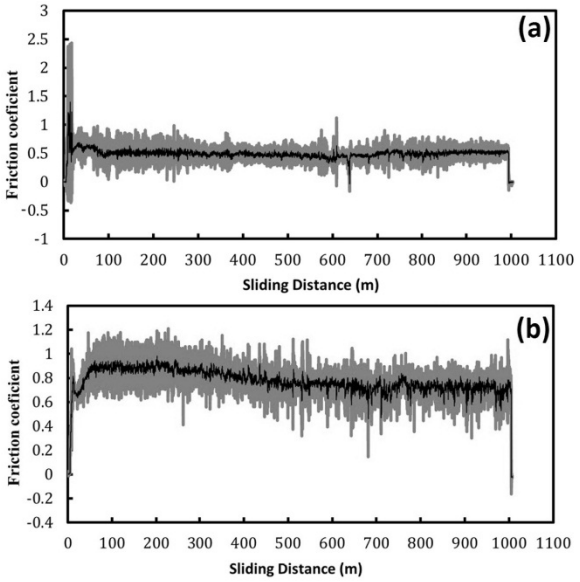


**Figure 11.** Friction coefficient evolution with sliding distance for (a) micro-structured and (b) nano-structured samples.

However, the story was rather different in nano-structured hard-metal. SEM images during sliding wear in nano-structured hard-metal are shown in Figure 13. After transition from steady-state, initial stage of nano-

structured hard-metal wear started (Figure 13a). Bright gray regions in the surface represented the worn zones. Afterward, these sections converted into scar islands (Figure 13b). Deep cracks and detached particles could be observed in scars (Figure 14a). Disconnections were formed in worn surface. Thereupon separate blocks were induced. Finally owing to compression between two surfaces, these blocks were converted into layers and delamination mechanism was activated (Figure 14b). Important visible observation was that continuity of composite was remained during the wear test.

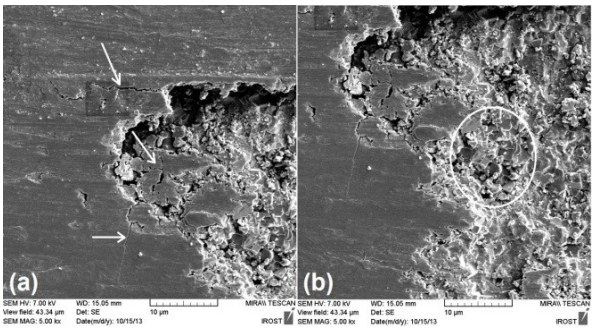


**Figure 12**. FE-SEM images of worn surface in micro-structured sample, (a) long cracks on worn surface, (b) disparted WC grains.

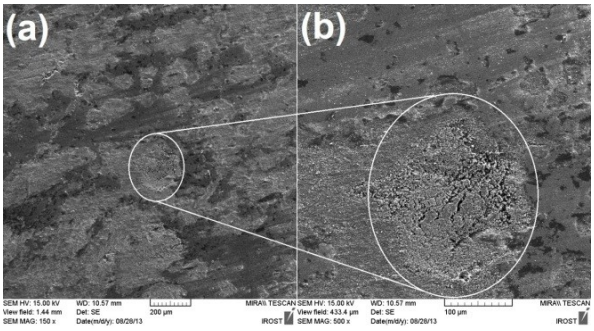


**Figure 13.** FE-SEM images of worn surfaces in nano-structured sample, (a) bright gray worn regions, (b) fragmentation in scar spot.

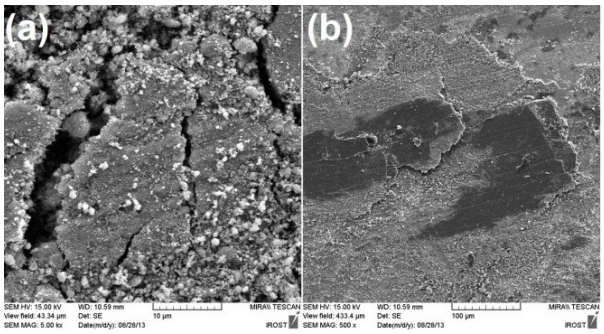


**Figure 14.** FE-SEM images of worn surfaces in nano-structured sample, (a) deep cracks in scar islands, (b) delamination on worn surface.

Basically whatever the hardness of worn surfaces is more, involvement between them will be greater and originally delamination phenomenon appertains to soft material, but other events occurred in these samples. Although wear mechanism in micro-structured cemented carbide began with removal of cobalt binder followed by abrasions and intergranular fracture and finished by fragmentation of carbide particles, in nano-structured cemented carbide, formation of fine abrasions followed by integrated flow and delamination was the main wear mechanism. The performance of the samples has been tested in actual machining process (Figure 15). In the same machining process, weight loss in nano structured sample at least 25% was lower than micro structured sample.

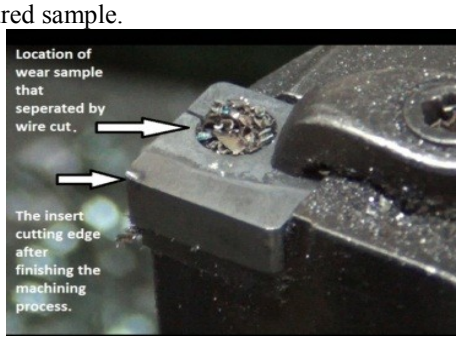


**Figure 15.** Image of nano structured sample after machining process.

Indeed wear mechanisms in hard-metals changed with WC particle size from micron to nano scale.

## 4. CONCLUSIONS

Comparison between wear behavior of micro-structured hard-metal and nano-structured hard-metal was regarded. The following conclusions were obtained:
Comparison between weight loss and images of wear scars showed that wear behavior was different in micro and nano-structured hard-metals. Studying numerical results of wear test determined that, in micro-structured hard-metal, weight loss was further than nano-structured hard-metal but mean friction coefficient and alteration of friction coefficient with distance were in less degree.
On the one hand finer WC particles in constant volume ultimately decreased mean free path, in contrary, presence of these nano-sized particles between two wear surfaces resulted in less demolition. Although involvement between worn surfaces in nano-structured hard-metal was more than that in micro-structured specimen, demolition was decreased. Abrasive wear mechanism was observed in both micro and nano-structured hard-metals. With proceeding in wear distance, deep cracks in nano-structured hard-metals were filled with delamination; but, in micro-structured hard-metals, deep cracks led to holes and broken blocks.

## 7. ACKNOWLEDGMENTS

The authors would like to acknowledge the financial support of Iran University of Science and Technology & …..

## REFERENCES


1. Liu, K., "Tungsten Carbide-Processing and Application", InTech, Croatia, (2012).
2. Cha, S.I. and Hong, S.H., "Hardness and fracture toughness of ultra-fine WC-10Co-X cemented carbides prepared from nanocrystalline powders", ***International Journal of Materials Research,*** Vol. 96, (2005), 172-176.
3. Michalski, A. and Siemiaszko, D., "Nano crystalline cemented carbides sintered by the pulse plasma method", I***nternational Journal of Refractory Metals and Hard Materials,*** Vol. 25, (2007), 153-158.
4. Querica, G., Grigorescu, I., Contreras, H., Rauso C.D. and Gutierrez-Campos D., "Friction and wear behavior of several hard materials", ***International Journal of Refractory Metals and Hard Materials,*** Vol. 19, (2001), 359-369.
5. Konyashin, I. and Ries, B., "Wear damage of cemented carbides with different combinations of WC mean grain size and Co content", ***International Journal of Refractory Metals and Hard Materials,*** Vol. 36, (2014), 12-19.
6. Rawat, S. and Attia, H., "Wear mechanisms and tool life management of WC–Co drills during dry high speed drilling of woven carbon fibre composites", ***Wear,*** Vol. 267, (2009), 1022-1030.
7. Picas, J.A., Xiong, Y., Punset, M., Ajdelsztajn, L., Forn, A. and Schoenung, M.J., "Microstructure and wear resistance of WC–Co by three consolidation processing techniques", ***International Journal of Refractory Metals and Hard Materials,*** Vol. 27, (2009), 344-349.
8. Bonny, K., Baets, P. D., Vleugels, J., Huang, S., Biest O.V.D. and Lauwers, B., "Impact of $Cr_3C_2$VC addition on the dry sliding friction and wear response of WC–Co cemented carbides", ***Wear,*** Vol. 267, (2009), 1642-1652.
9. Saito, H., Iwabuchi, A. and Shimizu, T., "Effects of Co content and WC grain size on wear of WC cemented carbide", ***Wear,*** Vol. 261, (2006), 126–132.
10. Shipway, P.H. and Hogg, J.J., "Dependence of micro scale abrasion mechanisms of WC-Co", ***Wear,*** Vol. 259, (2005), 44-51.
11. Allen, C., Sheen, M., Williams, J. and Pugsley, V.A., "The wear of ultrafine WC–Co hard metals", ***Wear***, Vol. 250, (2001), 604-610
12. Waseda, Y., Matsubara, E., Shinoda, K., "X-Ray Diffraction Crystallography Introduction- Examples and Solved Problems", Springer-Verlag Berlin Heidelberg, (2011).